RESEARCH ARTICLE

Adenosine monophosphate deaminase modulates BIN2 activity through hydrogen peroxide-induced oligomerization

Qing Lu[a,b], Anaxi Houbaert[a,b,d], Qian Ma[a,b], Jingjing Huang[a,b], Lieven Sterck[a,b], Cheng Zhang[a,b], René Benjamins[c], Frederik Coppens[a,b], Frank Van Breusegem[a,b], Eugenia Russinova[a,b,e]

[a]Department of Plant Biotechnology and Bioinformatics, Ghent University, 9052 Ghent, Belgium

[b]Center for Plant Systems Biology, VIB, 9052 Ghent, Belgium

[c]Plant Developmental Biology, Wageningen University Research, 6708 PB Wageningen, The Netherlands.

[d]Present address: Department of Plant Molecular Biology, Biophore, University of Lausanne, 1015 Lausanne, Switzerland

[e]Corresponding author: eurus@psb.ugent.be.

Short Title: H_2O_2 regulates BIN2 activity

One-sentence summary: A mutation in the *AMPD* gene reduces the sensitivity of Arabidopsis seedlings to brassinosteroids by modulating BIN2 oligomerization and activity in a hydrogen peroxide-dependent manner.

The author responsible for distribution of materials integral to the findings presented in this article in accordance with the policy described in the Instructions for Author (https://academic.oup.com/plcell) is: Eugenia Russinova (eugenia.russinova@psb.vib-ugent.be).

ABSTRACT

The *Arabidopsis thaliana* GSK3-like kinase, BRASSINOSTEROID-INSENSITIVE2 (BIN2) is a key negative regulator of brassinosteroid (BR) signaling and a hub for crosstalk with other signaling pathways. However, the mechanisms controlling BIN2 activity are not well understood. Here we performed a forward genetic screen for resistance to the plant-specific GSK3 inhibitor bikinin and discovered that a mutation in the *ADENOSINE MONOPHOSPHATE DEAMINASE (AMPD)/EMBRYONIC FACTOR1* (*FAC1)* gene reduces the sensitivity of Arabidopsis seedlings to both bikinin and BRs. Further analyses showed that AMPD modulates BIN2 activity by regulating its oligomerization in a hydrogen peroxide (H_2O_2)-dependent manner. Exogenous H_2O_2 induced the formation of BIN2 oligomers with a decreased kinase activity and an increased sensitivity to bikinin. By contrast, AMPD activity

inhibition reduces the cytosolic reactive oxygen species (ROS) levels and the amount of BIN2 oligomers, correlating with the decreased sensitivity of Arabidopsis plants to bikinin and BRs. Furthermore, we showed that BIN2 phosphorylates AMPD to possibly alter its function. Our results reveal the existence of a H_2O_2 homeostasis-mediated regulation loop between AMPD and BIN2 that fine-tunes the BIN2 kinase activity to control plant growth and development.

IN A NUTSHELL

Background: Brassinosteroids (BRs) are steroidal hormones that are essential for plant growth and development. BRs bind and activate the leucine-rich repeat receptor kinase BR INSENSITIVE1 (BRI1) and its coreceptor BRI1-ASSOCIATED KINASE1 (BAK1) to consequently inactivate the constitutively active GSK3-like kinase BR-INSENSITIVE2 (BIN2) and trigger BR responses. The synthetic chemical inhibitor of the plant GSK3-like kinases, bikinin can initiate BR signaling and is broadly used for functional studies of BR hormones.

Question: Although BR signaling pathway is well understood, not all mechanisms that control BIN2 activity are uncovered. Our aim was to find unknow BIN2 regulators via a forward genetic screen for bikinin-resistant mutants in Arabidopsis.

Findings: We discovered that a mutation in the *ADENOSINE MONOPHOSPHATE DEAMINASE* (*AMPD*)/*EMBRYONIC FACTOR1* (*FAC1*) gene reduces the sensitivity of Arabidopsis seedlings to both bikinin and BRs. Further studies showed that AMPD regulates BIN2 oligomerization by modulating the homeostasis of the reactive oxygen species (ROS) hydrogen peroxide (H_2O_2). The BIN2oligomer is less active and more sensitive to bikinin, compared to its monomer. In addition, BIN2 phosphorylates AMPD to possibly alter its function. Our study revealed a H_2O_2 homeostasis-mediated regulation loop between AMPD and BIN2 that fine-tunes the BIN2 kinase activity to control plant growth and development.

Next steps: We will further investigate how different types of ROS affect BIN2 activity and what roles these different mechanisms play in plant adaptation to the changing environment.

INTRODUCTION

Brassinosteroids (BRs) are a group of plant steroidal hormones that regulate diverse physiological and developmental processes (Kim and Russinova, 2020). In *Arabidopsis thaliana,* BR signaling is initiated with the perception of BRs by the receptor BR-INSENSITIVE1 (BRI1) (Wang et al., 2001) and its coreceptor BRI1-ASSOCIATED KINASE1 (BAK1) (Li et al., 2002; Nam and Li, 2002). A downstream phosphorylation/dephosphorylation cascade is triggered that inactivates the key negative regulator, the *Arabidopsis thaliana* Shaggy/GSK3-like kinase 21 (*At*SK21)/BR-INSENSITIVE2 (BIN2) (Vert and Chory, 2006; Kim et al., 2009), which phosphorylates and deactivates the transcription factors BRASSINAZOLE-RESISTANT1 (BZR1) (He et al., 2005) and BRI1-EMS-SUPPRESSOR1 (BES1)/BZR2 (Yin et al., 2002).

BIN2 and homologs are highly conserved serine/threonine kinases that, in addition to BR signaling, regulate many developmental and stress response pathways (Li et al., 2021; Mao et al., 2021). The BIN2 kinase activity is controlled by posttranslational modifications and protein-protein interactions (Mao and Li, 2020). For instance, tyrosine 200 (Tyr^{200}) phosphorylation is essential for the kinase activity of BIN2 (Kim et al., 2009). A kelch-repeat-containing phosphatase, BRI1-SUPPRESSOR1 (BSU1), inactivates BIN2 by dephosphorylating this conserved phospho-Tyr^{200} residue (Kim et al., 2009). In contrast, binding of the bZIP transcription factor ELONGATED HYPOCOTYL5 (HY5) to BIN2 enhances its activity by increasing the Tyr^{200} autophosphorylation (Li et al., 2020). Additionally, BIN2 phosphorylation at serine 187 (Ser^{187}) and Ser^{203} residues by the RIBOSOMAL PROTEIN S6 KINASE2 (S6K2) inhibits its kinase activity (Xiong et al., 2017). BIN2 is also inactivated by dephosphorylation at unknown residues by ABSCISIC ACID (ABA)-INSENSITIVE1 (ABI1) and ABI2, two type 2C serine/threonine phosphatases (PP2Cs) that play inhibitory roles in the ABA signaling pathway (Wang et al., 2018). Besides phosphorylation, the BIN2 kinase activity is regulated by acetylation at the lysine 189 (Lys^{189})

residue (Hao et al., 2016), S-nitrosylation at the cysteine 162 (Cys^{162}) residue (Wang et al., 2014) , and reactive oxygen species (ROS)-mediated oxidation at multiple Cys residues (Song et al., 2019). Furthermore, the F-box E3 ubiquitin ligase KINK SUPPRESSED IN BZR1-1D1 (KIB1)-induced ubiquitination promotes BIN2 degradation (Zhu et al., 2017).

Small molecules have been used widely to study BR biosynthesis and signaling (Dejonghe et al., 2014). For example, BRI1 and BIN2 have been identified via genetic screens for resistance to BRs that isolated their respective loss- and gain-of-function mutants (Clouse et al., 1996; Li et al., 2001). The BR biosynthesis inhibitor, brassinazole (BRZ) (Asami et al., 2000), has also played a key role in the discovery of the transcription factor BZR1 (Wang et al., 2002). Several other proteins involved in BR signaling in Arabidopsis, including BRZ-INSENSITIVE-LONG HYPOCOTYLS4 (BIL4) (Yamagami et al., 2009), BIL2 (Bekh-Ochir et al., 2013), and BRZ-SENSITIVE-SHORT HYPOCOTYL1 (BSS1) (Shimada et al., 2015) have been detected via forward genetic screens for altered sensitivity to BRZ. Another small molecule, bikinin, which inhibits the activity of BIN2 and seven other homologs by competing with adenosine 5'-triphosphate (ATP) (De Rybel et al., 2009), has been instrumental for the functional studies of BR signaling (Dejonghe et al., 2014) and its crosstalk with stomatal development (Houbaert et al., 2018), ABA signaling (Cai et al., 2014), phloem and xylem cell differentiation (Anne et al., 2015; Kondo et al., 2015; Tamaki et al., 2020), and root gravitropism (Retzer et al., 2019). However, unlike for BRs and BRZ, forward genetic screens for altered sensitivity to bikinin have not been reported.

Here, by means of a forward genetic screen for bikinin resistance, we identified seven mutants, designated *bikinin-resistant* (*bres*), that displayed a reduced sensitivity to bikinin and, to some extent, to the most active BR, brassinolide (BL). Mapping-by-sequencing and complementation analysis of two mutants, *bres1* and *bres2,* revealed that an identical recessive mutation in the *ADENOSINE MONOPHOSPHATE DEAMINASE (AMPD)*/*EMBRYONIC FACTOR1 (FAC1)* gene caused the bikinin resistance. AMPD maintains ATP catabolism and energy homeostasis by converting adenosine 5'-monophosphate (AMP) to inosine 5'-

monophosphate (IMP) (Han et al., 2006). We demonstrate that AMPD enhanced BIN2 oligomerization and consequently inhibited its activity in a hydrogen peroxide (H_2O_2)-dependent manner. Exogenous H_2O_2 induced the formation of BIN2 oligomers that were less active and more sensitive to bikinin *in vitro.* Genetic and pharmacological inhibition of AMPD decreased total ROS and H_2O_2 levels and reduced BIN2 oligomerization *in vivo*, respectively. In return, BIN2 might regulate the AMPD function and H_2O_2 production possibly through direct phosphorylation. Altogether, we uncovered an H_2O_2-dependent feedback mechanism for BIN2 activity regulation.

RESULTS

Forward genetic screen for bikinin resistance

To discover novel BR signaling components, we performed a forward genetic screen for resistance to the plant-specific GSK3 inhibitor, bikinin that induces constitutive BR responses in Arabidopsis (De Rybel et al., 2009). An EMS-mutagenized population of *PIN2p:PIN2-GFP*/Col-0 was used, but the presence of the transgene was not relevant to the screen. Approximately 10,000 M2 seeds, corresponding to 250 pools, were germinated and grown vertically on agar medium for 5 days. Next, the seedlings were positioned horizontally, overlaid with 30 ml liquid medium supplemented with 50 µM bikinin and grown additionally for 7 days in light. Bikinin-resistant plants were identified based on the lack of elongation growth of hypocotyls and petioles and by their darker green cotyledons (Supplemental Figure S1). The bikinin-resistant phenotype was validated by quantifying the hypocotyl length of the mutants in the M3 generation, when grown in the presence of 50 µM bikinin for 5 days in both light and dark. Seven mutants, designated *bres1* to *bres7*, failed to elongate their hypocotyls and petioles, indicating a reduced sensitivity to bikinin (Figure 1, A-D; Supplemental Figures S2, A-D). All 4-week-old *bres* mutants had smaller rosettes (Figure 1E; Supplemental Figure S2E). Whereas *bres3* and *bres4* displayed phenotypic traits typical of weak BR deficient mutants, such as compact rosette and dark-green leaves (Noguchi et al., 1999), *bres1* and *bres2* exhibited light-green-to-yellow rosette leaves (Figure 1E). As bikinin almost exclusively activates BR

signaling in Arabidopsis (De Rybel et al., 2009), the response to 100 nM BL was examined as well. All *bres* mutants were less sensitive to BL, albeit to variable degrees (Figure 1, A-D; Supplemental Figures S2, A-D). Moreover, *bres1* and *bres2* were hypersensitive to BRZ (Figure1, C and D). *bres1* and *bres2* were selected for further analysis.

Mutation in the *AMPD* gene reduced the sensitivity of Arabidopsis to bikinin and BRs

To identify the causative mutations for the bikinin resistance in *bres1* and *bres2*, we carried out a mapping-by-sequencing analysis (James et al., 2013), revealing a genetic linkage to a 3400-kb region on chromosome 2 for both mutants (Supplemental Figure S3A). By comparison with the whole-genome sequence of the parental *PIN2p:PIN2-GFP*/Col-0 line, the same point mutation in the *AMPD* gene, that resulted in the glycine-305-to-arginine conversion, was identified in the *bres1* and *bres2* mutants (Supplemental Figure S3, B and C).

To confirm that the bikinin resistance was caused by mutation in the *AMPD* gene, the 5.9 kb genomic *AMPD* fragment, including the promoter, was introduced into the *bres1* and *bres2* mutants. Similarly to the *PIN2p:PIN2-GFP*/Col-0 plants, the hypocotyls of the transgenic *AMPDp:gAMPD/bres1* and *AMPDp:gAMPD/bres2* Arabidopsis seedlings were elongated when grown in the presence of 50 μM bikinin (Supplemental Figure S3, D and E). Because of the zygote lethality of the known null *AMPD* mutants *fac1-1* and *fac1-2* (Xu et al., 2005) and of the fact that *bres1* and *bres2* mutations were located outside the AMPD domain (Supplemental Figure S3C), we concluded that they are weak mutants. As *bres2* displayed short and curled roots, which phenotype was not complemented by the *AMPD* gene (Supplemental Figure S3D), we used the *bres1* allele, hereafter indicated as *fac1-3*, for further study.

Next, we examined the sensitivity to bikinin and BL of wild type (accession Columbia-0 [Col-0]) plants in the presence of the synthetic modified nucleoside deaminoformycin (DF), an established inhibitor of AMPD (Lindell et al., 1999; Sabina et al., 2007). Similarly to the *fac1-3* mutant, wild type plants grown in the presence of DF (100 nM) were insensitive to bikinin and slightly hyposensitive to BL (Supplemental Figure S4, A-D) as assessed by their hypocotyl elongation. In agreement, when BES1 dephosphorylation was monitored as a readout for active

BR signaling (Yin et al., 2002), DF-treated plants showed a decreased BES1 dephosphorylation in the presence of exogenous BL (1-1000 nM) (Supplemental Figure S4, E and F), hinting at an impairment of the BR signaling. Altogether, our data demonstrate that the AMPD activity is required for bikinin and BR responses in Arabidopsis.

The impaired bikinin and BR responses in *fac1-3* are caused by the reduced H_2O_2 levels

Previously, the AMPD activity inhibition by DF in plants has been reported to increase the concentration of all adenosine ribonucleotides, including ATP (Sabina et al., 2007). Given that bikinin is an ATP-competitive kinase inhibitor (De Rybel et al., 2009), we hypothesized that ATP levels might be enhanced in *fac1-3*, explaining the bikinin insensitivity. However, treatment with the ATP synthesis inhibitor oligomycin (Krömer and Heldt, 1991) that reduces the ATP levels (Voon et al., 2018), did not restore the *fac1-3* sensitivity to 50 μM bikinin, as determined by their hypocotyl elongation (Supplemental Figure S5), suggesting that the bikinin insensitivity is not simply due to an ATP increase.

Activation of the mice AMPD3 stimulates ROS production (Hortle et al., 2016). Hence we speculated that the bikinin insensitivity of *fac1-3* might be caused by the reduced ROS levels in the mutant. To test this hypothesis, we examined whether exogenous ROS such as H_2O_2, would affect the *fac1-3* bikinin sensitivity. Although exogenous H_2O_2 generally inhibited seedling growth, the *fac1-3* sensitivity to 50 μM bikinin increased when grown on 1 or 2 mM H_2O_2 (Figure 2, A and B), implying that the impaired bikinin and BR responses in the *fac1-3* mutant might be due to altered H_2O_2 levels. To confirm that AMPD deficiency influences the ROS homeostasis in plants, we analyzed the H_2O_2 and total ROS levels by staining the *fac1-3* mutant with the fluorescent dyes H_2O_2-3′-O-acetyl-6′-O-pentafluorobenzenesulfonyl-2′-7′-difluorofluorescein-Ac (H_2O_2-BES-Ac) and 2',7'-dichlorodihydrofluorescein diacetate (H_2DCFDA), respectively. In support of our prediction, both H_2O_2 and total ROS were lower in *fac1-3* than those in the *PIN2p:PIN2-GFP*/Col-0 control but restored to wild type levels in the complemented *AMPDp:gAMPD/fac1-3* lines (Figure 2, C-F). Similarly, a 24-hour-treatment with 100 nM DF reduced both H_2O_2 and total ROS levels in Arabidopsis root tips

(Supplemental Figure S6, A-D).

As extracellular ATP (eATP) induces the accumulation of ROS in plants (Song et al., 2006; Chen et al., 2017), we tested whether an ATP application can rescue the bikinin and BL insensitivity of the *fac1-3* mutant. Notably, *fac1-3* restored its sensitivity to 50 μM bikinin and 100 nM BL, as indicated by the hypocotyl elongation and dephosphorylated BES1, when grown in the presence of 1 mM ATP (Figure 3, A-C). Next, we examined whether exogenous ATP could rescue *fac1-3* in terms of H_2O_2 homeostasis. Consistently, the H_2O_2 level was restored in *fac1-3* when treated with 1 mM ATP for 24 h (Figure 3, D and E). Considering that plant cells can take up adenosine, which is an ATP hydrolysis product in the apoplast, rather than absorb ATP directly (Scheerer et al., 2019), we checked whether adenosine could rescue *fac1-3* to exclude the possibility that eATP rescued *fac1-3* via an increased adenosine uptake. As hypothesized, *fac1-3* was still insensitive to 50 μM bikinin (Supplemental Figure S7) when grown in the presence of 0.5 mM exogenous adenosine. Moreover, given that the eATP elevates cytoplasmic ROS in a RESPIRATORY BURST OXIDASE HOMOLOGUE D (RBOHD)-dependent manner as a result of the activation of the plasma membrane receptors DOES NOT RESPOND TO NUCLEOTIDES1(DORN1)/PURINOCEPTOR P2K1 (P2K1) (Chen et al., 2017) and P2K2 (Pham et al., 2020), we tested whether P2K1 and RBOHD affected the bikinin response in Arabidopsis. In agreement, the *p2k1* and *rbohD/F* mutants were less sensitive to 50 μM bikinin in a hypocotyl elongation assay (Supplemental Figure S8). However, the sensitivity of *dorn1-3* and *rbohD/F* to bikinin was restored to that of the wild type when grown in the presence of 1 mM ATP (Supplemental Figure S8), possibly because the eATP-induced ROS production was not completely abolished in both mutants. Altogether, we conclude that the reduced endogenous H_2O_2 levels in *fac1-3* affect the insensitivity to bikinin and BRs.

H_2O_2-induced oligomerization of BIN2

Given that BIN2 is the direct target of bikinin (De Rybel et al., 2009), we examined the impact of H_2O_2 on the BIN2 protein *in vitro*. The bacterially produced and purified polyhistidine (HIS)-Small Ubiquitin-like Modifier (SUMO)-tagged BIN2 protein was treated with H_2O_2 and then

analyzed with non-reducing sodium dodecyl sulfate-polyacrylamide gel electrophoresis (SDS-PAGE). BIN2 monomer, dimer, and oligomer bands were detected (Figure 4A). Moreover, the multiple band pattern of HIS-SUMO-BIN2 on SDS-PAGE was reversed by the addition of the reducing agent dithiothreitol (DTT) (Figure 4A). Consistently, the size-exclusion chromatography (SEC) analysis also revealed the existence of BIN2 oligomers after treatment with 5 mM H_2O_2 (Figure 4B).

It was previously shown that several BIN2 Cys residues are prone to oxidation (Song et al., 2019), hence we checked whether these residues are involved in the formation of oxidation-dependent oligomer formation of BIN2. Consequently, five Cys residues, Cys^{59}, Cys^{95}, Cys^{99}, Cys^{162} and Cys^{267} in BIN2 were substituted with Ser to generate $BIN2^{5CS}$. The oligomerization of HIS-SUMO-$BIN2^{5CS}$ by H_2O_2 was completely abolished (Figure 4C), whereas BIN2 with individual mutations in Cys^{59}, Cys^{162}, and the double $Cys^{95,99}$ mutation still was oligomerized by H_2O_2 (Figure 4D). Even though only two of the tested Cys residues, Cys^{59} and Cys^{162}, are conserved in the ten BIN2 homologs (Supplemental Figure S9A), we examined whether H_2O_2 also induced the formation of protein oligomers for all *At*SKs and found that, similarly to BIN2, the monomer, dimer, and oligomer bands were detected as well (Supplemental Figure S9B). Thus, H_2O_2 caused oligomerization of BIN2 and its homologs, most likely by inducing the formation of intermolecular disulfide bonds.

Next, we tested whether the oligomeric state of BIN2 affected its kinase activity and bikinin sensitivity by means of an *in vitro* kinase assay with oligomer and monomer proteins of HIS-SUMO-BIN2, which had eluted from the SEC column, and with the BES1-tagged maltose-binding protein (MBP-BES1) as a substrate. Both the BIN2 oligomer and monomer were able to phosphorylate MBP-BES1, but its phosphorylation by the BIN2 monomer was higher than that of the BIN2 oligomer (Figure 4E). Furthermore, 20 µM bikinin completely blocked the BIN2 monomer-mediated MBP-BES1 phosphorylation, but only slightly reduced the phosphorylation of MBP-BES1 by the BIN2 oligomer (Figure 4E). The kinase assay indicated that oligomerization reduced the kinase activity of BIN2 and increased its sensitivity to bikinin.

To check whether BIN2 forms oligomers *in vivo*, we first examined the BIN2 protein self-interaction using fluorescence lifetime imaging microscopy (FLIM) to determine Förster resonance energy transfer (FRET), indicative of BIN2 homodimerization in *Nicotiana benthamiana* leaf epidermis. The fluorescence lifetime of BIN2-GFP was significantly reduced when co-expressed with BIN2-mCherry but not when together with either BIN2^{5CS}-mCherry or the PLASMA MEMBRANE INTRINSIC PROTEIN 2A (PIP2A)-mCherry that was used as a negative control (Supplemental Figure S10), demonstrating that BIN2 can form oligomers in a cysteine-dependent manner *in vivo*. To further confirm this, we expressed the GFP-tagged BIN2 and BIN2^{5CS} under the control of the native promoter in *bin2-3*. We detected both monomer and oligomer for BIN2-GFP, whereas only the monomer was detected for BIN2^{5CS}-GFP (Figure 4F). In addition, treatment with 100 nM DF for 24 h reduced the amount of BIN2 oligomer (Figure 4, F and G).

Given that heat stress induces ROS (Schwarzländer et al., 2009; Babbar et al., 2021), we examined whether high temperature treatment will affect the BIN2 oligomeric status. As expected, the ratio of BIN2 oligomer to total BIN2 protein was increased after heating at 42°C for 1 h (Figure 4, F and G). Then we investigated if BIN2 activity *in vivo* is affected by the Cys mutations. To this end, we compared how overexpression of BIN2-GFP and BIN2^{5CS}-GFP at the same transcript levels affected the plant growth. The *bin2-3* plants overexpressing BIN2^{5CS}-GFP displayed more severe dwarf phenotypes compared with plants overexpressing BIN2-GFP, (Figure 4G, Supplemental Figure S11), suggesting that BIN2^{5CS}-GFP is more active *in vivo*. Altogether, our data indicate that AMPD regulates BIN2 kinase activity and sensitivity to bikinin through H_2O_2-induced oligomerization.

BIN2 phosphorylates the AMPD protein *in vitro*

Because the phosphorylation intensities of AMPD were reduced in Arabidopsis cell suspensions treated with bikinin (Lu et al., 2022), we explored the possibility that AMPD is a direct substrate of BIN2 and its homologs. Co-immunoprecipitation experiments in *Nicotiana benthamiana* leaf epidermis transiently expressing AMPD-GFP and *At*SKs-HA revealed that AMPD co-

immunoprecipitated with nine of the ten *At*SK proteins (Figure 5A). In addition, HIS-SUMO-BIN2 phosphorylated *in vitro* the truncated protein HIS-SUMO-AMPD$^{32-839}$, which lacks the first 31 amino acid residues of the transmembrane domain (Figure 5B). Because mutation of AMPD reduced the levels of total ROS and H_2O_2 in Arabidopsis, we examined whether bikinin and BL can influence the H_2O_2 homeostasis. Similar to a previous report that BRs trigger the production of ROS (Tian et al., 2018), the H_2O_2 levels were increased in root tips of *PIN2p:PIN2-GFP*/Col-0 seedlings grown in the presence of 50 μM bikinin and 100 nM BL for 24 hours (Figure 5, C and D). However, in *fac1-3*, bikinin could not increase the H_2O_2 levels while BL induced-H_2O_2 increase was partially inhibited (Figure 5, C and D). Altogether, our data showed that *At*SKs might regulate H_2O_2 homeostasis via AMPD.

DISCUSSION

BR signaling involves inactivation of BIN2 and homologs (Vert and Chory, 2006; Kim et al., 2009). The activity of BIN2 is regulated by different mechanisms, including posttranslational modifications and protein-protein interactions (Mao and Li, 2020; Li et al., 2021). Here, we showed that AMPD modulates BIN2 activity and BR signaling, by H_2O_2-induced oligomerization. Genetic or pharmacological inhibition of AMPD reduced the ROS and H_2O_2 levels in Arabidopsis, leading to reduced BIN2 oligomer formation causing a complete insensitivity to bikinin and to a lesser degree resistance to BRs. In turn, BIN2 and homologs coimmunoprecipitated and phosphorylated AMPD, suggesting that in addition to other mechanisms (Li et al., 2014; Lv et al., 2018; Tian et al., 2018; Yan et al., 2020) BRs partly regulate ROS levels through controlling AMPD function. Therefore, in the *fac1-3* mutant, BIN2 inhibition by bikinin did not induce H_2O_2, whereas BRs, which inhibit the BIN2 activity indirectly, induced H_2O_2, albeit less than in the control. The difference between bikinin and BRs in terms of H_2O_2 production in *fac1-3* might account for the different sensitivity of the mutant to bikinin and BRs. Altogether, our study provides a novel feedback mechanism for control of BIN2 activity and respectively BR signaling by H_2O_2-induced BIN2 oligomerization (Figure 6).

In mice blood cells, AMPD3 activation depleted ATP and increased ROS production (Hortle et al., 2016). Similarly, pharmacological inhibition of Arabidopsis AMPD increases the intracellular amounts of ATP (Sabina et al., 2007) and when the AMPD function was impaired the endogenous ROS and H_2O_2 levels were reduced (Figure 2). It remains unclear how AMPD regulates ROS and H_2O_2 homeostasis. However, because the energy homeostasis affects ROS production (Suzuki et al., 2012) we can speculate that AMPD regulates ROS in an energy-dependent manner. Moreover, pharmacological inhibition or deletion of human AMPD led to the activation of AMP-activated protein kinase (AMPK) in skeletal muscles (Plaideau et al., 2014) and the AMPK activity could limit the mitochondrial ROS production (Rabinovitch et al., 2017). Considering that Arabidopsis AMPD localizes in the mitochondrial outer membranes (Duncan et al., 2011), it might also influence the ROS production through modulation of the mitochondrial function. In plants, eATP induce ROS through the plasma membrane NADPH oxidase (Sagi and Fluhr, 2006; Kim et al., 2006; Chen et al., 2017). We also observed that eATP increased H_2O_2 levels in both *PIN2p:PIN2-GFP*/Col-0 and *fac1-3* roots. The fact that the increased H_2O_2 production either by stimulating the eATP signaling or by providing exogenous H_2O_2 partially restored the sensitivity to bikinin in *fac1-3* indicates that AMPD regulates the activity of GSK3-like kinases and the plant response to bikinin as well as to BRs through ROS.

Oligomerization is a well-known phenomenon that occurs in both eukaryotic and prokaryotic organisms and the protein oligomeric status is important for regulation of protein activity (Kumari and Yadav, 2019). In plants, protein oligomerization is implicated in immunity (Mou et al., 2003) and the auxin signaling pathway (Dezfulian et al., 2016). In addition, the oligomeric association of the kelch-repeat-containing BSU family phosphatases that inactivated BIN2 is also required for the regulation of their function as well as the effective BR signaling (Kim et al., 2016). The oligomerization is controlled by various processes, including the ROS-induced formation of disulfide bonds (Chi et al., 2013). For example, H_2O_2 regulates the oligomeric status of a set of Arabidopsis proteins, such as the basic leucine zipper (bZIP) transcription factor *At*bZIP16 (Shaikhali et al., 2012) and the essential regulator of plant systemic acquired resistance NONEXPRESSER OF PR GENES1 (NPR1) (Mou et al., 2003).

Here, we found that H_2O_2 induced the oligomerization of BIN2 and of its homologs as well via the formation of disulfide bonds between certain Cys residues among. The fact that only Cys^{59} and Cys^{162} are conserved in all *At*SKs might suggests that these two Cys residues are essential for GSK3 oligomerization. Furthermore, we demonstrated that DF treatment prohibited the formation of BIN2 oligomer, and the BIN2 monomer was less sensitive to the GSK3 inhibitor, bikinin, than the BIN2 oligomer, possibly the reason for the insensitivity to bikinin of *fac1-3* or DF-treated Col-0 plants. It has been shown that heat stress induces ROS accumulation (Schwarzländer et al., 2009; Babbar et al., 2021) and BES1 dephosphorylation (Albertos et al., 2022). In agreement, heat treatment increased the levels of BIN2 oligomer that was less active than the BIN2 monomer, indicating BIN2 oligomerization might be involved in the heat stress-induced BES1 dephosphorylation. Altogether, our data revealed an unknown mechanism for the regulation of the BR signaling via H_2O_2.

Previous studies have shown that S-nitrosylation on Cys^{162} of BIN2 could reduce the kinase activity (Wang et al., 2014), whereas the singlet oxygen ($^1O_2$), one of the ROS, activates BIN2 and promotes its association with BES1 by oxidation of the cysteine residues Cys^{59}, Cys^{95}, Cys^{99}, and Cys^{162} (Song et al., 2019). However, we found that H_2O_2-induced oligomerization represses the BIN2 activity. In plants, ROS have different production and processing systems. For example, $^1O_2$ is mainly generated in the chloroplast photosystem II (PSII), whereas H_2O_2 can be produced in various organelles, such as peroxisomes, chloroplasts, mitochondria, cytosol, and apoplast (Mhamdi and Van Breusegem, 2018). Each type of ROS has a different oxidative capacity and affects diverse physiological and biochemical reactions regulated by various genes in plants (Phua et al., 2021). Therefore, the involvement of H_2O_2 and $^1O_2$ in the BIN2 activity control might be important for plants to adapt to distinctive environmental conditions. In addition to the regulation of the BIN2 activity, ROS oxidize BZR1 and enhance its transcriptional activity by promoting its interaction with AUXIN RESPONSE FACTOR6 (ARF6) and PHYTOCHROME INTERACTING FACTOR4 (PIF4) (Tian et al., 2018). Notably, the thioredoxin protein, TRXh5, could reduce BZR1 (Tian et al., 2018), but which thioredoxin protein is involved in the BIN2 regulation remains to be uncovered. Together, our data suggest

a complex mechanism for ROS control of BR signaling that might be vital for plants to respond to different environmental stimuli.

As AMPD plays an important role in adenine nucleotides metabolism and the energy homeostasis, its function is regulated by different mechanisms (Dieni and Storey, 2008). In Arabidopsis, it has been shown that ATP activates the AMPD via binding to its Walker A motif (residues 289–296) (Han et al., 2006). The glycine^{305} that is converted to Alanine in *fac1-3* localizes near the Walker A motif while the aspartic acid^{508} that is converted to asparagine in *fac1-1* localizes in the middle of the AMP deaminase domain (Xu et al., 2005), probably explaining why *fac1-1* is embryonic lethal and *fac1-3* is a weak mutant. Moreover, it was reported that the activity of animal AMPD is regulated by phosphorylation (Tovmasian et al., 1990; Thakkar et al., 1993; Dieni and Storey, 2008). Similarly, our data revealed that AMPD was phosphorylated by *At*SKs *in vitro*. In addition, previous study showed that the phosphorylation intensities of seven residues (Tyr^{70}, Ser^{73}, Ser^{76}, Ser^{134}, Ser^{140}, Ser^{203}, Thr^{280}) were reduced by bikinin in Arabidopsis cell suspensions (Lu et al., 2022), indicating that the GSK3-like kinases might regulate AMPD function through phosphorylation.

In conclusion, we revealed a regulatory mechanism of BIN2 activity and BR signaling in an AMPD-H_2O_2-dependent manner. However, it remains to be discovered how BIN2 regulates the AMPD function *in vivo*. When considering the different roles of ROS on the regulation of various BR signaling components, it will be necessary to determine how these mechanisms control plant growth and environmental responses cooperatively.

MATERIALS AND METHODS

Plant materials and growth conditions

The following mutants and transgenic *Arabidopsis thaliana* (L. Heynh.) lines have been described previously: *PIN2p:PIN2-GFP/*Col-0 (Abas et al., 2006), *p2k1* (Choi et al., 2014), *rbohD/F* (Torres et al., 2005) and *bin2-3* was obtained from a backcross of the triple *bin2-3/atsk22/atsk2*3 mutant (Vert and Chory, 2006) into Col-0 (Gudesblat et al., 2012). Arabidopsis seeds were stratified for 2 days at 4°C, germinated, and grown on half-strength Murashige and

Skoog (½MS) agar plates containing 1% (w/v) sucrose at 22°C and a 16 h-8-h light-dark photoperiod for 5 days under 120 µmol m^{-2} s^{-1} of photosynthetically active radiation with LED light bulbs (OSRAM L36W/840). Plants grown for 4 weeks were transferred to soil at day 6. *Nicotiana benthamiana* plants were grown in the greenhouse under a 14-h light (93 µmol m−2 s−1)/10-h dark regime at 25°C.

Generation of constructs

To generate the *35Sp:AMPD-GFP*, the coding sequence (CDS) of *AMPD* (*AT2G32820*) without a stop codon was amplified and introduced into the *pDONR221* vector. The entry clones, *pDONR221-AMPD*, *pDONRP4-P1Rp35Sp*, and *pDONRP2R-P3-EGFP* (Karimi et al., 2002) were recombined in a multisite LR reaction with *pH7m34GW* (Invitrogen) as the destination vector. To generate the *35Sp:AtSKs-HA* constructs of the 10 *AtSKs*, the entry vectors *pDONR221-AtSKs* (Houbaert et al., 2018) were recombined with *pDONRP4-P1R-35Sp*, *pDONRP2R-P3-HA*, and *pH7m34GW* with the multisite LR reaction. To generate the *AMPDp:AMPD* construct, the genomic fragment of *AMPD* including its promoter (-924bp to 5026 bp from the start codon) was amplified and introduced into *pDONR221* vector and was recombined with the *pH7WG* destination vector in the LR reaction. The resulting construct *AMPDp:AMPD* was introduced into *bres1* and *bres2*. To generate the *BIN2p:BIN2-GFP* and *BIN2p:BIN2^{5CS}-GFP* constructs, the *pDONR221-BIN2^{5CS}* was made by the one-step PCR-based mutagenesis method (Liu and Naismith, 2008) using a *pDONR221-BIN2* (Houbaert et al., 2018) as a template. The entry clones, *pDONR221-BIN2* or *pDONR221-BIN2^{C5S}*, *pDONRP4-P1R-35Sp* and *pDONRP2R-P3-EGFP* (Karimi et al., 2002) were recombined in a multisite LR reaction with *pH7m34GW* (Invitrogen) as the destination vector. The resulting constructs *BIN2p:BIN2-GFP* and *BIN2p:BIN2^{5CS}-GFP* were introduced into *bin2-3*. To generate the constructs used for protein purification, the CDS of the 10 *AtSKs* were amplified and introduced into a *pET-SUMO* vector (Yang et al., 2017) by means of the Gibson cloning method. The *pET-HIS-SUMO-BIN2^{C59S}*, *pET-HIS-SUMO-BIN2$^{C95S/C99S}$*, *pET-HIS-SUMO-BIN2^{C162S}*, and *pET-HIS-SUMO-BIN2^{5CS}* were generated by the one-step PCR-based mutagenesis method (Liu and

Naismith, 2008). The CDS of *AMPD* without the first 93 nucleotides (AMPD$^{32-839}$) was amplified and introduced into the *pET-HIS-SUMO* vector with the Gibson cloning method. The CDS of *BES1* was amplified and introduced into the entry vector *pDONR221*. The *pDONR221-BES1* was recombined with the destination vector *pDEST-HIS-MBP* (Invitrogen) to generate the expression clone *pDEST-HISMBP-BES1*. All the primers used are listed in Supplemental Table S1. All clones were confirmed by sequencing.

Whole genome sequencing and mutation mapping

The two mutants, *bres1* and *bres2*, were backcrossed with the parental *PIN2p:PIN2-GFP*/Col-0 line and the subsequent F2 generation was used for genotyping. Plants that showed a bikinin resistant phenotype in terms of hypocotyl elongation when grown in the presence of 50 µM bikinin were selected and grown further. One true leaf from at least 100 screened plants each was harvested and pooled for genomic DNA extraction. As an internal reference, DNA from the parental *PIN2p:PIN2-GFP*/Col-0 line originally used for EMS mutagenesis was also extracted. Next-generation sequencing was performed on the Illumina NextSeq500 instrument (Mid Output v2.5, 300 bp, Paired Reads; VIB Nucleomics Core). The mutations were mapped with SHOREmap (v.2.0) (Schneeberger et al., 2009) using the *A. thaliana* genome as a reference (TAIR10, Col-0). A 3.4 kb-region on chromosome 2 for both mutants was identified with genetic linkage to both the *bres1* and *bres2* mutants. The whole genome comparison between the *bres* mutants and the parental *PIN2p:PIN2-GFP*/Col-0 revealed the same point mutation in the *AMPD* gene in the two *bres* mutants.

Chemical treatments

ATP (500 mM stock in H_2O) (Sigma-Aldrich), adenosine (250 mM stock in H_2O) (Sigma-Aldrich), bikinin (50 mM stock in DMSO) (homemade), BL (10 mM stock in DMSO) (Wako Pure Chemical Industries), brassinazole (10 mM stock in DMSO) (TCI EUROPE), H_2O_2 (Merck Millipore), MG132 (150 mM stock in DMSO) (Sigma-Aldrich) and deaminoformycin (10 mM stock in H_2O) (Bayer CropScience GmbH) were used at the indicated concentrations.

Immunoblot

The Arabidopsis seedlings were ground in liquid nitrogen, resuspended in total protein extraction buffer (25 mM Tris-HCl, pH 7.5, 150 mM NaCl, and Roche cOmplete ULTRA protease inhibitor cocktail, Roche PhosSTO tablet) in a 1:2 (w/v) ratio, and centrifuged at 15,000g. The supernatants were mixed with the required amount of 4× NuPAGE LDS sample buffer (Invitrogen) and 10× NuPAGE sample-reducing agent (Invitrogen), heated at 70°C for 10 min, and loaded onto 4-20% Mini-PROTEAN TGX precast gels. The proteins were transferred to polyvinylidene fluoride membranes by means of the Trans-Blot® Turbo™ Transfer System (Bio-Rad). The membranes were probed with the anti-BES1 antibody (Yin et al., 2002). The secondary antibodies were the enhanced chemiluminescence (ECL) α-rabbit IgG, horseradish peroxidase (HRP)-linked whole antibody (GE-Healthcare). Blots were developed with the Western Lightning Plus-ECL, ECL Substrate (Perkin-Elmer), and imaged with the ChemiDoc XRS+ molecular imager (Bio-Rad). Intensity of protein bands was measured with the Bio-Rad Image Lab software package.

Co-immunoprecipitation

Agrobacterium tumefaciens strain C58, carrying the constructs of interest were co-infiltrated with a p19-harboring strain in the abaxial side of *Nicotiana benthamiana* leaves. After 48 h of infiltration, the total proteins were isolated with extraction buffer (20 mM Tris-HCl pH 7.5, 150 mM NaCl, 10 mM dithiothreitol [DTT], 1% [v/v] NP-40, 1 cOmplete protease inhibitor [Sigma-Aldrich]) in a 1:2 (w/v) ratio. The lysates were incubated with GFP-Trap magnetic agarose beads (Chromotek) for 2 h at 4°C. The beads were collected with a DynaMag™-2 Magnetic separation rack and washed three times with washing buffer (20 mM Tris-HCl pH 7.5, 150 mM NaCl, 0.5% [v/v] NP-40). The enriched proteins were released from the beads by boiling in NuPAGE™ LDS Sample Buffer and analyzed by immunoblots with α-GFP-HRP and α-HA-HRP antibodies according to the immunoblot protocol.

Protein purification

Constructs for HIS-SUMO-BIN2 and HIS-SUMO-AMPD$^{32-839}$ were transformed in competent

Escherichia coli BL21 (DE3) pLysS cells. The transformed cells were cultured in Luria-Bertani medium supplemented with carbenicillin (100 mg/mL) at 37°C. Expression was induced by the addition of 0.2 mM isopropyl β-D-1-thiogalactopyranoside at 16°C overnight. Cells were harvested by centrifugation at 6000*g*, resuspended in lysis buffer (1.06 mM NaH_2PO_4, 18.94 mM Na_2HPO_4, 300 mM NaCl, 5 mM DTT, 0.1% [m/v] (3-((3-cholamidopropyl) dimethylammonio)-1-propanesulfonate [CHAPS], 10% [v/v] glycerol, pH 8.0), supplemented with protease inhibitors (Roche), and lysed by sonication. Recombinant proteins were purified with a HIS-Trap FF 5-ml column (GE-Healthcare) and further purified by size-exclusion chromatography with a preparative grade HiLoad 16/600 Superdex 200 column (GE-Healthcare) with the elution buffer (1.06 mM NaH_2PO_4, 18.94 mM Na_2HPO_4, 300 mM NaCl, 0.1% [m/v] CHAPS, 10% [v/v] glycerol, pH 8.0).

In vitro kinase assay

For the experiments for HIS-SUMO-BIN2 monomer and oligomer with MBP-BES1, HIS-SUMO-BIN2 monomer proteins (20 μM) was incubated with 5 mM H_2O_2 at room temperature for 30 min, and then both protein monomer and oligomer were separated by size-exclusion chromatography with a preparative grade Superdex 200 Increase 10/300 GL column (GE-Healthcare) with the elution buffer (1.06 mM NaH_2PO_4, 18.94 mM Na_2HPO_4, 300 mM NaCl, 0.1% [m/v] CHAPS, 10% [v/v] glycerol, pH 8.0). Recombinant proteins required were incubated in the kinase reaction buffer (50 mM Tris-HCl, pH 7.5, 100 mM NaCl, 10 mM $MgCl_2$, and 10 μM adenosine 5'-triphosphate) at the presence of 5 μCi [γ-^{32}P]-ATP (NEG502A001MC; Perkin-Elmer) at 25°C for 60 min. The reactions were terminated by adding NuPAGE LDS sample buffer (Invitrogen) and NuPAGE sample-reducing agent (Invitrogen), separated on 4-20% SDS-PAGE, and stained with Coomassie Brilliant Blue. Gels were dried and radioactivity was detected by autoradiography on a photographic film with an FLA 5100 phosphor imager (Fujifilm).

In vitro oligomerization analysis

Each HIS-SUMO-*At*SK (20 μM) was incubated with 5 mM H_2O_2 at room temperature for

30 min. For the protein electrophoresis analysis, the H_2O_2-treated proteins were mixed with the required amount of 5× non-reducing protein sample buffer (250 mM Tris-HCl, 50% [v/v] glycerol, 10% [v/v] SDS, 0.25% [v/v] bromophenol blue, pH 6.8) or the protein sample buffer with extra 20 mM DTT, heated at 70°C for 10 min, and loaded onto 4-20% Mini-PROTEAN TGX precast gels. The protein gels were stained with Coomassie Brilliant Blue. For the size-exclusion chromatography analysis, 400 µl H_2O_2-treated HIS-SUMO-BIN2 proteins were analyzed with the AKTA machine with Superdex® 200 Increase 10/300 GL column (GE-Healthcare).

In vivo oligomerization analysis

Five-day-old Arabidopsis seedlings of *BIN2p:BIN2-GFP* and *BIN2p:BIN2^{C5S}-GFP* were treated with H_2O (mock), 100 nM DF for 24 h with 10 µM MG132 co-treatment or heated at 42 ℃ for 1 h after 23h of 10 µM MG132 pre-treatment in liquid 1/2 medium. After treatments, the proteins were ground, resuspended in extraction buffer containing -SH blocking agent iodoacetamide (25 mM Tris-HCl, pH 7.5, 150 mM NaCl, 30 µM iodoacetamide and Roche cOmplete ULTRA protease inhibitor cocktail) in a 1:2 (w/v) ratio, incubated at room temperature for 30 min, and centrifuged at 15,000g. The supernatants were mixed with the required amount of NuPAGE™ LDS Sample Buffer with 10 mM DTT (reducing condition) or without DTT (non-reducing condition) and analyzed by immunoblot with α-GFP-HRP antibody.

Fluorescence Resonance Energy Transfer by fluorescence lifetime imaging

Agrobacterium tumefaciens strain C58, carrying the constructs of interest were co-infiltrated with a p19-harboring strain in the abaxial side of *Nicotiana benthamiana* leaves. After 3 d of infiltration, FRET-FLIM experiments were carried out using a Olympus FluoView FV1000 confocal installed with the fluorescence lifetime system (PicoQuant SymPhoTime version 2.4.4874). The fluorescence lifetime of BIN2-GFP when expressed alone was used as the negative control. The average and standard error of different fluorescent lifetime were calculated from at least 10 independent measurements, and the significance of the result was

analyzed by One-way ANOVA.

ROS and H_2O_2 staining

The 5-day-old Arabidopsis seedlings were incubated either with 50 µM CM-H_2DCFDA (Thermo Fisher) or H_2O_2-BES-Ac (FUJIFILM Wako) in liquid ½MS medium for 30 min for ROS and H_2O_2, respectively. After a brief wash with the medium, the roots were observed under a fluorescence microscope. Whole-root staining was imaged with an inverted confocal laser scanning microscope (Leica SP8 LIGHTNING confocal microscope) with 488 nm excitation. Emission was detected between 517 to 527 nm for ROS and 515 to 530 nm for H_2O_2. The signal intensities were measured with Image J (version 1.53f51).

Reverse Transcription quantitative-PCR

Total RNA was extracted from 100 mg plant material with the ReliaPrep™ RNA Tissue Miniprep System (Promega). cDNA was generated with the qScript cDNA SuperMix (Quantabio). The *BIN2* and *EF1a* genes were amplified with SYBR green I qPCR master mix (Roche) and LightCycler 480 (Roche). All primers are listed in Supplemental Table S1.

Quantification and statistical analysis

All statistical analyses were carried out in Graphpad Prism (version 9.0.1). Significant differences were determined with ANOVA analysis or the Student's *t*-test as indicated (Supplemental Data Set S1). Quantification of hypocotyl lengths or fluorescence signal intensities were presented as individual value plots with whiskers representing means and s.d.

Accession Numbers

Accession numbers of genes reported in this study include: AT2G38280 (AMPD/FAC1), AT5G26751 (AtSK11), AT3G05840 (AtSK12), AT5G14640 (AtSK13), AT4G18710 (AtSK21/BIN2), AT1G06390 (AtSK22), AT2G30980 (AtSK23), AT3G61160 (AtSK31), AT4G00720 (AtSK32), AT1G09840 (AtSK41), AT1G57870 (AtSK42) and AT1G19350 (BES1). The whole genome sequencing data is submitted to the European Nucleotide Archive

(ENA) as PRJEB49127.

Supplemental Data

Supplemental Figure S1. Schematic illustration of the forward genetic screen for bikinin-resistant mutants.

Supplemental Figure S2. Phenotypes of the *bikinin-resistant3* (*bres3*) to *bres7* mutants.

Supplemental Figure S3. *AMPD* rescued *bres1* and *bres2.*

Supplemental Figure S4. Pharmacological inhibition of AMPD reduced the sensitivity of Arabidopsis to bikinin and BL.

Supplemental Figure S5. Adenosine triphosphate (ATP) production inhibition by oligomycin did not restore the *fac1-3* sensitivity to bikinin.

Supplemental Figure S6. Pharmacological inhibition of AMPD reduced ROS levels.

Supplemental Figure S7. Adenosine treatment did not restore the *fac1-3* sensitivity to bikinin.

Supplemental Figure S8. *p2k1* and *rbohD/F* mutants are less sensitive to bikinin.

Supplemental Figure S9. Hydrogen peroxide-induced oligomerization of the GSK3-like kinases *in vitro*.

Supplemental Figure S10. BIN2-GFP interacts with BIN2-mCherry but not $BIN2^{5CS}$-mCherry.

Supplemental Figure S11. Reverse transcription quantitative PCR analysis of *BIN2* expression level

Supplemental Table S1. Primers used.

Supplemental Data Set S1. Statistical analysis

Acknowledgements

We thank Kiwamu Tanaka (Washington State University) for providing the *dorn1-3* and *rhohDF* seeds and for valuable suggestions; Stephen Lindell (Bayer CropScience) for providing deaminoformycin; Evelien Mylle and Yaowei Wang (VIB-Ghent University) for the help with FRET-FLIM, Balkan Canher (VIB-Ghent University) for the help with the mutant screen; Jonah

Nolf and Savvas Savvides (VIB-Ghent University) for help with the protein purification; Yanhai Yin (Iowa State University) for providing the anti-BES1 antibody; Johan Winne and Brenda Callebaut (Ghent University) for synthesizing bikinin; Torsten Möhlmann (University Kaiserslautern) for valuable suggestions and Martine De Cock (VIB-Ghent University) for help in preparing the manuscript.

Funding

Q.L. and C.Z. are indebted to the China Scholarship Council for predoctoral fellowships and J.H. is the recipient of a senior postdoctoral fellowship of the Research Foundation-Flanders (G1227020N). The work was supported by Research Foundation-Flanders (projects no G009018N and no. G002121N) to E.R.

Conflict of interest statement. The authors declare that they have no conflict of interest.

Author contributions

Q.L., A.H. and E.R. conceived the project. R.B. provided the EMS mutant population. A.H. designed the screen, identified the mutants and backcrossed them to the parental line. Q. L., L.S., and F.C. performed the Shore mapping analysis. Q.L. did cloning, phenotypic analysis, BES1 dephosphorylation assay, protein work and ROS analysis. Q.L. and C.Z. performed the kinase assay. Q.M. performed FRET-FLIM, Q.L., Q.M., J.H., and F.V.B. performed the oligomerization assay. Q.L. and E.R. wrote the manuscript. All authors revised the manuscript.

References

Abas L, Benjamins R, Malenica N, Paciorek T, Wiśniewska J, Moulinier-Anzola JC, Sieberer T, Friml J, Luschnig C (2006) Intracellular trafficking and proteolysis of the *Arabidopsis* auxin-efflux facilitator PIN2 are involved in root gravitropism. Nat Cell Biol **8:** 249–256

Albertos, P, Dündar, G, Schenk, P, Carrera, S, Cavelius, P, Sieberer, T, Poppenberger, B (2022) Transcription factor BES1 interacts with HSFA1 to promote heat stress

resistance of plants. EMBO J. **41**: e108664

Anne P, Azzopardi M, Gissot L, Beaubiat S, Hématy K, Palauqui J-C (2015) OCTOPUS negatively regulates BIN2 to control phloem differentiation in *Arabidopsis thaliana*. Curr Biol **25:** 2584–2590

Asami, T, Min, YK, Nagata, N, Yamagishi, K, Takatsuto, S, Fujioka, S, Murofushi, N, Yamaguchi, I, Yoshida, S (2000) Characterization of Brassinazole, a Triazole-Type Brassinosteroid Biosynthesis Inhibitor. Plant Physiol **123**: 93–100

Babbar, R, Karpinska, B, Grover, A, Foyer, CH (2021) Heat-Induced Oxidation of the Nuclei and Cytosol. Front. Plant Sci. **11**: 617779

Bekh-Ochir D, Shimada S, Yamagami A, Kanda S, Ogawa K, Nakazawa M, Matsui M, Sakuta M, Osada H, Asami T, et al (2013) A novel mitochondrial DnaJ/Hsp40 family protein BIL2 promotes plant growth and resistance against environmental stress in brassinosteroid signaling. Planta **237:** 1509–1525

Cai Z, Liu J, Wang H, Yang C, Chen Y, Li Y, Pan S, Dong R, Tang G, de Dios Barajas-Lopez J, et al (2014) GSK3-like kinases positively modulate abscisic acid signaling through phosphorylating subgroup III SnRK2s in *Arabidopsis*. Proc Natl Acad Sci USA **111:** 9651–9656

Chen D, Cao Y, Li H, Kim D, Ahsan N, Thelen J, Stacey G (2017) Extracellular ATP elicits DORN1-mediated RBOHD phosphorylation to regulate stomatal aperture. Nat Commun **8:** 2265

Chi Y-H, Paeng S-K, Kim M-J., Hwang G-Y, Melencion SM, Oh H-T, Lee S-Y (2013) Redox-dependent functional switching of plant proteins accompanying with their structural changes. Front. Plant Sci. **4:** 277

Choi J, Tanaka K, Cao Y, Qi Y, Qiu J, Liang Y, Lee SY, Stacey G (2014) Identification of a plant receptor for extracellular ATP. Science **343:** 290–294

Clouse SD, Langford M, McMorris TC (1996) A brassinosteroid-insensitive mutant in Arabidopsis thaliana exhibits multiple defects in growth and development. Plant Physiol **111:** 671–678

De Rybel B, Audenaert D, Vert G, Rozhon W, Mayerhofer J, Peelman F, Coutuer S, Denayer T, Jansen L, Nguyen L, et al (2009) Chemical inhibition of a subset of *Arabidopsis thaliana* GSK3-like kinases activates brassinosteroid signaling. Chem Biol **16:** 594–604

Dejonghe W, Mishev K, Russinova E (2014) The brassinosteroid chemical toolbox. Curr Opin Plant Biol **22:** 48–55

Dezfulian MH, Jalili E, Roberto DKA, Moss BL, Khoo K, Nemhauser JL, Crosby WL (2016) Oligomerization of SCF^{TIR1} is essential for Aux/IAA degradation and auxin signaling in Arabidopsis. PLoS Genet **12:** e1006301

Dieni CA, Storey KB (2008) Regulation of 5'-adenosine monophosphate deaminase in the freeze tolerant wood frog, Rana sylvatica. BMC Biochem **9:** 12

Duncan O, Taylor NL, Carrie C, Eubel H, Kubiszewski-Jakubiak S, Zhang B, Narsai R, Millar AH, Whelan J (2011) Multiple lines of evidence localize signaling, morphology, and lipid biosynthesis machinery to the mitochondrial outer membrane of Arabidopsis. Plant Physiol **157:** 1093–1113

Gudesblat GE, Schneider-Pizoń J, Betti C, Mayerhofer J, Vanhoutte I, Van Dongen W, Boeren S, Zhiponova M, De Vries S, Jonak C, Russinova E (2012) SPEECHLESS integrates brassinosteroid and stomata signalling pathways. Nat. Cell Biol. **14:** 548-554

Han BW, Bingman CA, Mahnke DK, Bannen RM, Bednarek SY, Sabina RL, Phillips Jr GN (2006) Membrane association, mechanism of action, and structure of *Arabidopsis* embryonic factor 1 (*FAC1*). J Biol Chem **281:** 14939–14947

Hao Y, Wang H, Qiao S, Leng L, Wang X (2016) Histone deacetylase HDA6 enhances brassinosteroid signaling by inhibiting the BIN2 kinase. Proc Natl Acad Sci USA **113:** 10418–10423

He J-X, Gendron JM, Sun Y, Gampala SSL, Gendron N, Sun CQ, Wang Z-Y (2005) BZR1 is a transcriptional repressor with dual roles in brassinosteroid homeostasis and growth responses. Science **307:** 1634–1638

Hortle E, Nijagal B, Bauer DC, Jensen LM, Ahn SB, Cockburn IA, Lampkin S, Tull D,

McConville MJ, McMorran BJ, et al (2016) Adenosine monophosphate deaminase 3 activation shortens erythrocyte half-life and provides malaria resistance in mice. Blood **128:** 1290–1301

Houbaert A, Zhang C, Tiwari M, Wang K, de Marcos Serrano A, Savatin DV, Urs MJ, Zhiponova MK, Gudesblat GE, Vanhoutte I, et al (2018) POLAR-guided signalling complex assembly and localization drive asymmetric cell division. Nature **563:** 574-578

James GV, Patel V, Nordström KJV, Klasen JR, Salomé PA, Weigel D, Schneeberger K (2013) User guide for mapping-by-sequencing in *Arabidopsis*. Genome Biol **14:** R61

Karimi M, Inzé D, Depicker A (2002) GATEWAY™ vectors for *Agrobacterium*-mediated plant transformation. Trends Plant Sci **7:** 193-195

Kim E-J, Russinova E (2020) Brassinosteroid signalling. Curr Biol **30:** R294-R298

Kim E-J, Youn J-H, Park C-H, Kim T-W, Guan S, Xu S, Burlingame AL, Kim Y-P, Kim S-K, Wang Z-Y, et al (2016) Oligomerization between BSU1 family members potentiates brassinosteroid signaling in *Arabidopsis*. Mol Plant **9:** 178-181

Kim S-Y, Sivaguru M, Stacey G (2006) Extracellular ATP in plants. Visualization, localization, and analysis of physiological significance in growth and signaling. Plant Physiol **142:** 984-992

Kim T-W, Guan S, Sun Y, Deng Z, Tang W, Shang J-X, Sun Y, Burlingame AL, Wang Z-Y (2009) Brassinosteroid signal transduction from cell-surface receptor kinases to nuclear transcription factors. Nat Cell Biol **11:** 1254-1260

Kondo Y, Fujita T, Sugiyama M, Fukuda H (2015) A novel system for xylem cell differentiation in *Arabidopsis thaliana*. Mol Plant **8:** 612-621

Krömer S, Heldt HW (1991) On the role of mitochondrial oxidative phosphorylation in photosynthesis metabolism as studied by the effect of oligomycin on photosynthesis in protoplasts and leaves of barley (*Hordeum vulgare*). Plant Physiol **95:** 1270-1276

Kumari N, Yadav S (2019) Modulation of protein oligomerization: an overview. Prog Biophys Mol Biol **149:** 99-113

Li C, Zhang B, Yu H (2021) GSK3s: nodes of multilayer regulation of plant development and stress responses. Trends Plant Sci **26:** 1286-1300

Li J, Nam KH, Vafeados D, Chory J (2001) BIN2, a new brassinosteroid-insensitive locus in Arabidopsis. Plant Physiol **127:** 14-22

Li J, Terzaghi W, Gong Y, Li C, Ling J-J, Fan Y, Qin N, Gong X, Zhu D, Deng XW (2020) Modulation of BIN2 kinase activity by HY5 controls hypocotyl elongation in the light. Nat Commun **11:** 1592

Li J, Wen J, Lease KA, Doke JT, Tax FE, Walker JC (2002) BAK1, an *Arabidopsis* LRR receptor-like protein kinase, interacts with BRI1 and modulates brassinosteroid signaling. Cell **110:** 213-222

Li L, Li M, Yu L, Zhou Z, Liang X, Liu Z, Cai G, Gao L, Zhang X, Wang Y, et al (2014) The FLS2-associated kinase BIK1 directly phosphorylates the NADPH oxidase RbohD to control plant immunity. Cell Host Microbe **15:** 329-338

Lindell SD, Moloney BA, Hewitt BD, Earnshaw CG, Dudfield PJ, Dancer JE (1999) The design and synthesis of inhibitors of adenosine 5′-monophosphate deaminase. Bioorg. Med. Chem. Lett **9:** 1985-1990

Liu H, Naismith JH (2008) An efficient one-step site-directed deletion, insertion, single and multiple-site plasmid mutagenesis protocol. BMC Biotechnol **8:** 91

Lu Q, Zhang Y, Hellner J, Xu X, Pauwels J, Giannini C, Ma Q, Dejonghe W, Han H, Van de Cotte B, et al (2022) Proteome-wide cellular thermal shift assay reveals unexpected cross-talk between brassinosteroid and auxin signaling. Proc Natl Acad Sci USA **119**: e2118220119

Lv B, Tian H, Zhang F, Liu J, Lu S, Bai M, Li C, Ding Z (2018) Brassinosteroids regulate root growth by controlling reactive oxygen species homeostasis and dual effect on ethylene synthesis in *Arabidopsis*. PLoS Genet **14:** e1007144

Mao J, Li J (2020) Regulation of three key kinases of brassinosteroid signaling pathway. Int J Mol Sci **21:** 4340

Mao J, Li W, Liu J, Li J (2021) Versatile physiological functions of plant GSK3-like kinases.

Genes **12:** 697

Mhamdi A, Van Breusegem F (2018) Reactive oxygen species in plant development. Development **145:** dev.164376

Mou Z, Fan W, Dong X (2003) Inducers of plant systemic acquired resistance regulate NPR1 function through redox changes. Cell **113:** 935-944

Nam KH, Li J (2002) BRI1/BAK1, a receptor kinase pair mediating brassinosteroid signaling. Cell **110:** 203-212

Noguchi T, Fujioka S, Choe S, Takatsuto S, Yoshida S, Yuan H, Feldmann KA, Tax FE (1999) Brassinosteroid-insensitive dwarf mutants of Arabidopsis accumulate brassinosteroids. Plant Physiol **121:** 743-752

Pham AQ, Cho S-H, Nguyen CT, Stacey G (2020) Arabidopsis lectin receptor kinase P2K2 is a second plant receptor for extracellular ATP and contributes to innate immunity. Plant Physiol **183:** 1364-1375

Phua SY, De Smet B, Remacle C, Chan KX, Van Breusegem F (2021) Reactive oxygen species and organellar signaling. J. Exp. Bot **72:** 5807-5824

Plaideau C, Lai Y-C, Kviklyte S, Zanou N, Löfgren L, Andersén H, Vertommen D, Gailly P, Hue L, Bohlooly-Y M, et al (2014) Effects of pharmacological AMP deaminase inhibition and *Ampd1* deletion on nucleotide levels and AMPK activation in contracting skeletal muscle. Chem Biol **21:** 1497-1510

Rabinovitch RC, Samborska B, Faubert B, Ma EH, Gravel S-P, Andrzejewski S, Raissi TC, Pause A, St.-Pierre J, Jones RG (2017) AMPK maintains cellular metabolic homeostasis through regulation of mitochondrial reactive oxygen species. Cell Rep **21:** 1-9

Retzer K, Akhmanova M, Konstantinova N, Malínská K, Leitner J, Petrášek J, Luschnig C (2019) Brassinosteroid signaling delimits root gravitropism via sorting of the *Arabidopsis* PIN2 auxin transporter. Nat Commun **10:** 5516

Sabina RL, Paul A-L, Ferl RJ, Laber B, Lindell SD (2007) Adenine nucleotide pool perturbation is a metabolic trigger for AMP deaminase inhibitor-based herbicide toxicity.

Plant Physiol **143:** 1752-1760

Sagi M, Fluhr R (2006) Production of reactive oxygen species by plant NADPH oxidases. Plant Physiol **141:** 336-340

Scheerer U, Trube N, Netzer F, Rennenberg H, Herschbach C (2019) ATP as phosphorus and nitrogen source for nutrient uptake by *Fagus sylvatica* and *Populus* x *canescens* roots. Front Plant Sci **10:** 378

Schneeberger K, Ossowski S, Lanz C, Juul T, Petersen AH, Nielsen KL, Jørgensen JE, Weigel D, Andersen SU (2009) SHOREmap: simultaneous mapping and mutation identification by deep sequencing. Nat. Methods **6**: 550-551

Schwarzländer, M, Fricker, MD, Sweetlove, LJ (2009) Monitoring the in vivo redox state of plant mitochondria: Effect of respiratory inhibitors, abiotic stress and assessment of recovery from oxidative challenge. Biochim. Biophys. Acta BBA - Bioenerg. **1787**: 468–475

Shaikhali J, Norén L, de Dios Barajas-López J, Srivastava V, König J, Sauer UH, Wingsle G, Dietz K-J, Strand Å (2012) Redox-mediated mechanisms regulate DNA binding activity of the G-group of basic region leucine zipper (bZIP) transcription factors in *Arabidopsis*. J Biol Chem **287:** 27510-27525

Shimada S, Komatsu T, Yamagami A, Nakazawa M, Matsui M, Kawaide H, Natsume M, Osada H, Asami T, Nakano T (2015) Formation and dissociation of the BSS1 protein complex regulates plant development via brassinosteroid signaling. Plant Cell **27:** 375-390

Song CJ, Steinebrunner I, Wang X, Stout SC, Roux SJ (2006) Extracellular ATP induces the accumulation of superoxide via NADPH oxidases in Arabidopsis. Plant Physiol **140:** 1222-1232

Song S, Wang H, Sun M, Tang J, Zheng B, Wang X, Tan Y-W (2019) Reactive oxygen species-mediated BIN2 activity revealed by single-molecule analysis. New Phytol **223:** 692-704

Suzuki N, Koussevitzky S, Mittler R, Miller G (2012) ROS and redox signalling in the

response of plants to abiotic stress. Plant Cell Environ **35:** 259-270

Tamaki T, Oya S, Naito M, Ozawa Y, Furuya T, Saito M, Sato M, Wakazaki M, Toyooka K, Fukuda H, et al (2020) VISUAL-CC system uncovers the role of GSK3 as an orchestrator of vascular cell type ratio in plants. Commun Biol **3:** 184

Thakkar JK, Janero DR, Yarwood C, Sharif HM (1993) Modulation of mammalian cardiac AMP deaminase by protein kinase C-mediated phosphorylation. Biochem. J **291:** 523-527

Tian Y, Fan M, Qin Z, Lv H, Wang M, Zhang Z, Zhou W, Zhao N, Li X, Han C, et al (2018) Hydrogen peroxide positively regulates brassinosteroid signaling through oxidation of the BRASSINAZOLE-RESISTANT1 transcription factor. Nat Commun **9:** 1063

Torres MA, Jones JDG, Dangl JL (2005) Pathogen-induced, NADPH oxidase–derived reactive oxygen intermediates suppress spread of cell death in *Arabidopsis thaliana*. Nat Genet **37:** 1130-1134

Tovmasian EK, Hairapetian RL, Bykova EV, Severin SE, Haroutunian AV (1990) Phosphorylation of the skeletal muscle AMP-deaminase by protein kinase C. FEBS Lett **259:** 321-323

Vert G, Chory J (2006) Downstream nuclear events in brassinosteroid signalling. Nature **441:** 96-100

Voon CP, Guan X, Sun Y, Sahu A, Chan MN, Gardeström P, Wagner S, Fuchs P, Nietzel T, Versaw WK, et al (2018) ATP compartmentation in plastids and cytosol of *Arabidopsis thaliana* revealed by fluorescent protein sensing. Proc Natl Acad Sci USA **115:** E10778-E10787

Wang H, Tang J, Liu J, Hu J, Liu J, Chen Y, Cai Z, Wang X (2018) Abscisic Acid signaling inhibits brassinosteroid signaling through dampening the dephosphorylation of BIN2 by ABI1 and ABI2. Mol Plant **11:** 315-325

Wang P, Du Y, Hou Y-J, Zhao Y, Hsu C-C, Yuan F, Zhu X, Tao WA, Song C-P, Zhu J-K (2014) Nitric oxide negatively regulates abscisic acid signaling in guard cells by S-nitrosylation of OST1. Proc Natl Acad Sci USA **112:** 613-618

Wang Z-Y, Nakano T, Gendron J, He J, Chen M, Vafeados D, Yang Y, Fujioka S, Yoshida S, Asami T, et al (2002) Nuclear-localized BZR1 mediates brassinosteroid-induced growth and feedback suppression of brassinosteroid biosynthesis. Dev Cell **2:** 505-513

Wang Z-Y, Seto H, Fujioka S, Yoshida S, Chory J (2001) BRI1 is a critical component of a plasma-membrane receptor for plant steroids. Nature **410:** 380-383

Xiong F, Zhang R, Meng Z, Deng K, Que Y, Zhuo F, Feng L, Guo S, Datla R, Ren M (2017) Brassinosteriod Insensitive 2 (BIN2) acts as a downstream effector of the Target of Rapamycin (TOR) signaling pathway to regulate photoautotrophic growth in Arabidopsis. New Phytol **213:** 233-249

Xu J, Zhang H-Y, Xie C-H, Xue H-W, Dijkhuis P, Liu C-M (2005) *EMBRYONIC FACTOR 1* encodes an AMP deaminase and is essential for the zygote to embryo transition in Arabidopsis. Plant J **42:** 743-758

Yamagami A, Nakazawa M, Matsui M, Tujimoto M, Sakuta M, Asami T, Nakano T (2009) Chemical genetics reveal the novel transmembrane protein BIL4, which mediates plant cell elongation in brassinosteroid signaling. Biosci Biotechnol Biochem **73:** 415-421

Yan M-Y, Xie D-L, Cao J-J, Xia X-J, Shi K, Zhou Y-H, Zhou J, Foyer CH, Yu J-Q (2020) Brassinosteroid-mediated reactive oxygen species are essential for tapetum degradation and pollen fertility in tomato. Plant J **102:** 931-947

Yang Z, Qiu Q, Chen W, Jia B, Chen X, Hu H, He K, Deng X, Li S, Tao WA, Cao X, Du J (2017) Structure of the Arabidopsis JMJ14-H3K4me3 Complex Provides Insight into the Substrate Specificity of KDM5 Subfamily Histone Demethylases. Plant Cell **30:** 167-177

Yin Y, Wang Z-Y, Mora-Garcia S, Li J, Yoshida S, Asami T, Chory J (2002) BES1 accumulates in the nucleus in response to brassinosteroids to regulate gene expression and promote stem elongation. Cell **109:** 181-191

Zhu J-Y, Li Y, Cao D-M, Yang H, Oh E, Bi Y, Zhu S, Wang Z-Y (2017) The F-box protein KIB1 mediates brassinosteroid-induced inactivation and degradation of GSK3-like kinases in *Arabidopsis*. Mol Cell **66:** 648-657

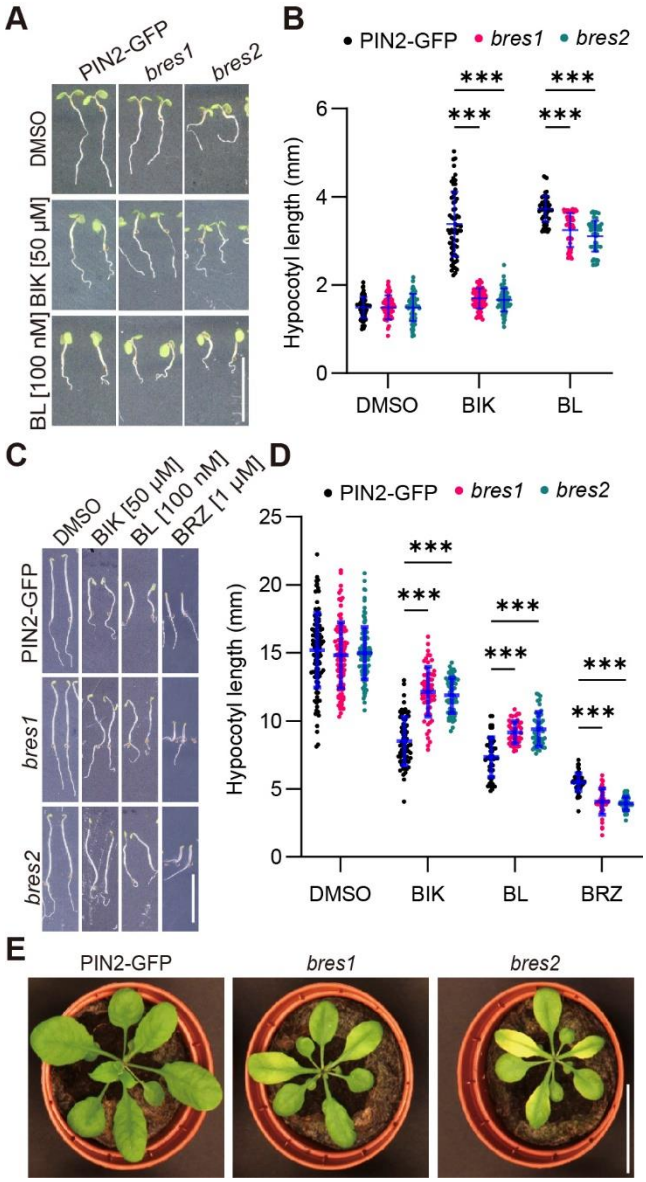

Figure 1 *bres1* and *bres2* mutants are insensitive to bikinin and brassinolide but hypersensitive to brassinazole. A and C, Arabidopsis seedlings of *bres1*, *bres2*, and the parental line *PIN2p:PIN2-GFP/*Col-0 were germinated and grown for 5 days on agar medium supplemented with 50 µM bikinin (BIK), 100 nM brassinolide (BL), or DMSO (mock) under long-day conditions (16 h light/8 h dark cycle) (A) and on agar medium supplemented with the same chemicals as in (A) and 1 µM brassinazole (BRZ) in dark (C). B and D, Quantification of the hypocotyl length of genotypes presented in (A) and (C). Scatter dot plots show all the individual points with the means and standard errors. *P* values compared to *PIN2p:PIN2-GFP/*Col-0 plants. Two-way ANOVA with Dunnett's multiple comparisons test was used, ***$P < 0.001$. $n \geq 40$ seedlings from three independent experiments. E, Phenotypes of the *bres1* and *bres2* mutants and the control, *PIN2p:PIN2-GFP/*Col-0, grown in soil for 4 weeks. Scale bars, 1 cm (A) and (C), 2 cm (E)

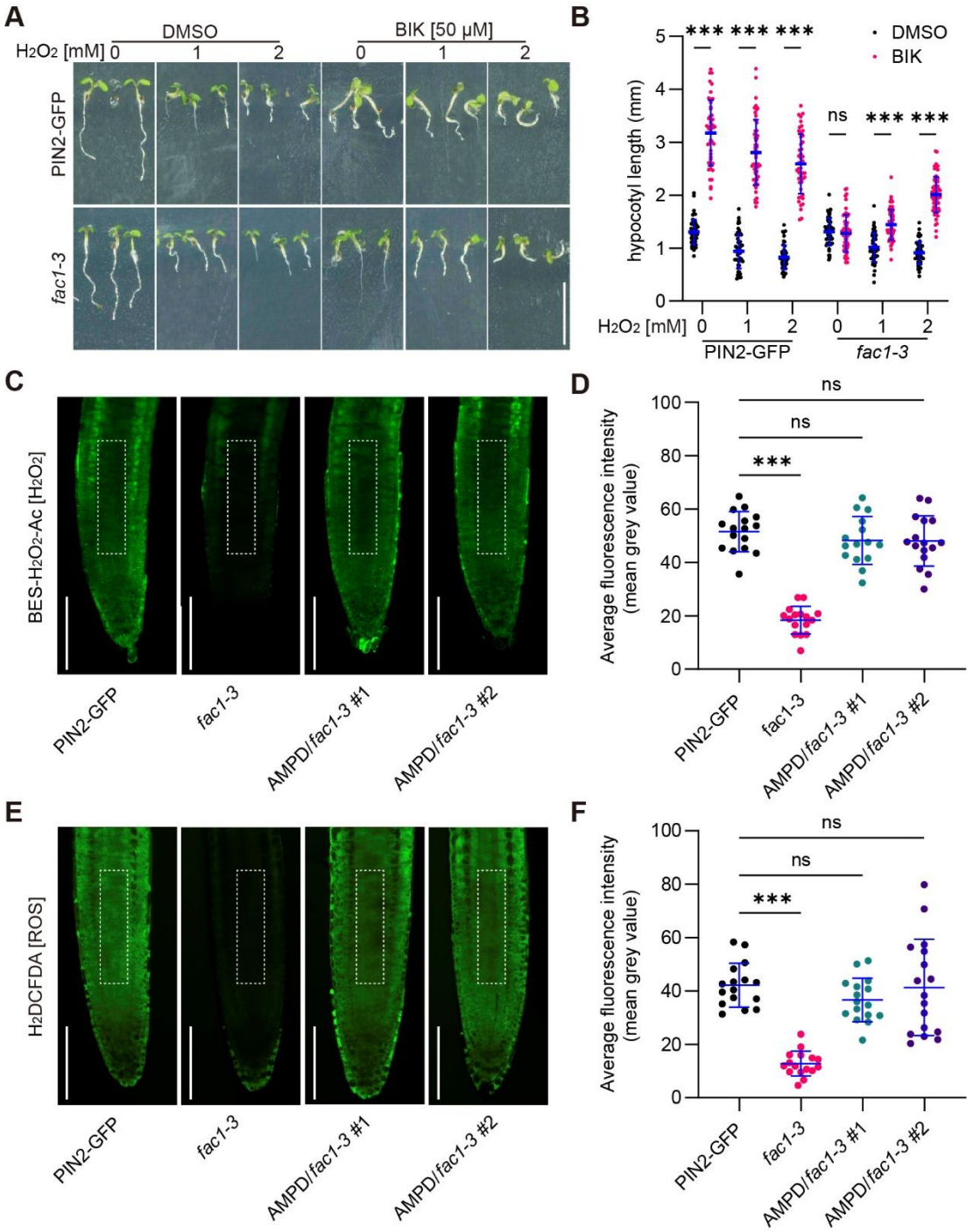

Figure 2 H2O2 dependence of the *fac1*-3 sensitivity to bikinin. A, Arabidopsis seedlings of *fac1-3* and *PIN2p:PIN2-GFP/*Col-0 germinated and grown for 5 days on agar medium supplemented with 1 mM and 2 mM H_2O_2 in the presence of 50 µM bikinin (BIK) or DMSO (mock). B, Quantification of the hypocotyl length of seedlings in (A). *P* values compared to *PIN2p:PIN2-GFP/*Col-0. Two-way ANOVA with Dunnett's multiple comparisons test was used, ***$P < 0.001$, ns, not significant. $n \geq 40$ seedlings from three independent experiments. C and E, Confocal images of root tips of 5-day-old seedlings of *PIN2p:PIN2-GFP/*Col-0, *fac1-3* and two independent transgenic lines *AMPDp:gAMPD/fac1-3* stained with the H_2O_2 probe H_2O_2-BES-Ac (C) and the ROS probe 2′,7′-dichlorodihydrofluorescein diacetate (H_2DCFDA) (E). The white frames indicate the region used for quantification. D and F, Quantification of the fluorescent intensities in the root tips of the seedlings in (C) and (E). *n*, at least 15 seedlings from three independent experiments. *P* values compared to *PIN2p:PIN2-GFP/*Col-0. One-way ANOVA with Dunnett's post hoc test was used, ***$P < 0.001$. ns, not significant. B, D, and F, Scatter dot plots show all the individual points with the means and standard errors. Scale bars, 1 cm (A), 100 µm (C and E).

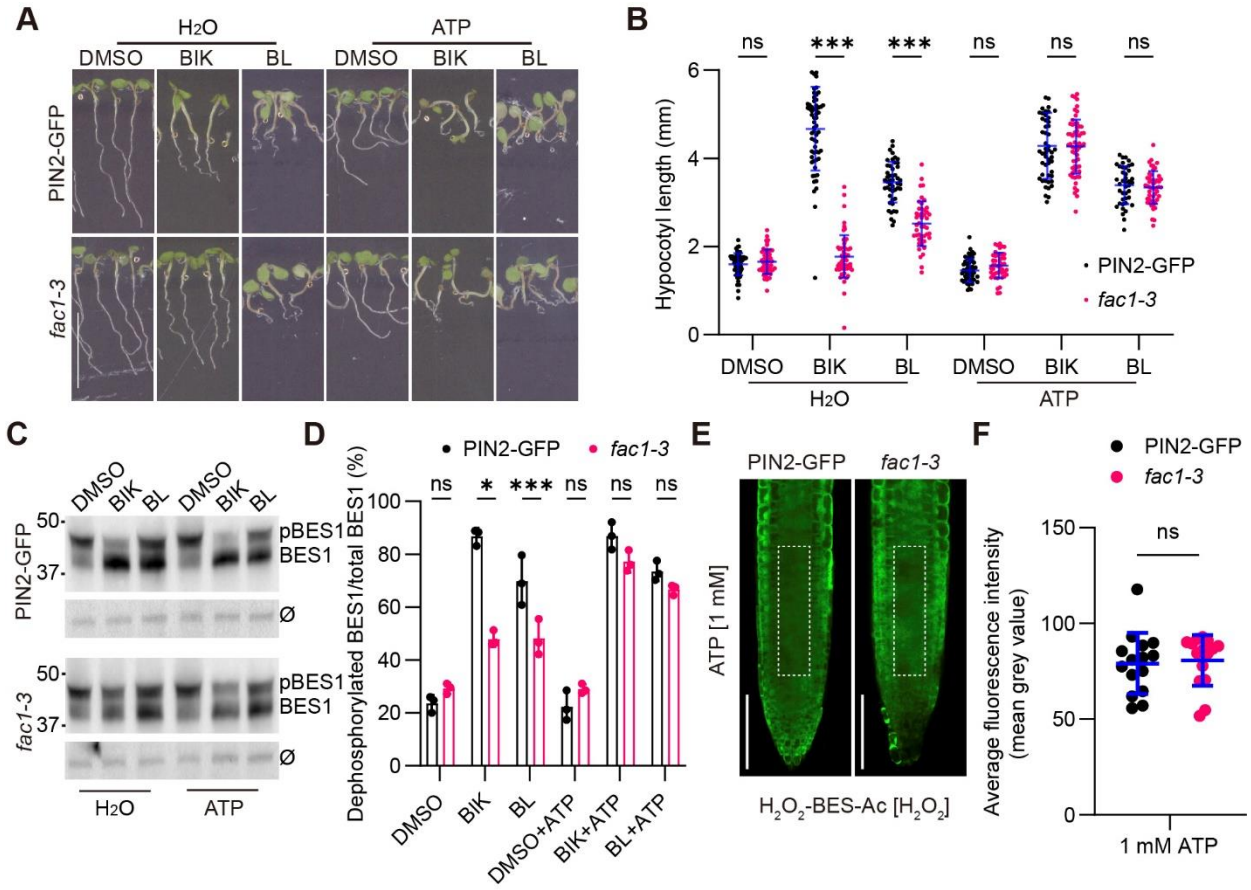

Figure 3 Exogenous ATP restored the *fac1-3* sensitivity to bikinin and BRs. A, Arabidopsis seedlings of *fac1-3* and *PIN2p:PIN2-GFP*/Col-0 germinated and grown for 5 days on agar medium supplemented with 1 mM ATP or H2O (mock for ATP) and in the presence of 50 µM bikinin (BIK), 100 nM brassinolide (BL), or DMSO (mock for BIK and BL). B, Quantification of the hypocotyl length of seedlings in (A). *P* values compared to *PIN2p:PIN2-GFP*/Col-0 plants. Two-way ANOVA with Dunnett's multiple comparisons test was used, ***$P < 0.001$; ns, not significant. $n \geq 40$ seedlings from three independent experiments. C, Immunoblot analysis of BES phosphorylation of seedlings in (A) with a specific anti-BES1 antibody. pBES1, phosphorylated BES1; Ø, unspecific bands used as a control. D, Quantification of the ratio between dephosphorylated BES1 and total BES1. Bar chart shows the means and standard errors. *P* values compared to PIN2-GFP. Two-way ANOVA with Dunnett's multiple comparisons test was used, *$P < 0.05$; ***$P < 0.001$; ns, not significant. *n*, three independent experiments. E, Confocal images of root tips of 5-day-old *PIN2p:PIN2-GFP*/Col-0 and *fac1-3* seedlings stained with the H_2O_2 probe H_2O_2-BES-Ac. The white frames indicate the region used for quantification. F, Quantification of the fluorescence intensity in the root tips in (D). *n*, at least 15 seedlings from three independent experiments. *P* values compared to *PIN2p:PIN2-GFP*/Col-0 (Student's *t*-test). ns, not significant. B and F, Scatter dot plots show all the individual points with the means and standard errors. Scale bars, 1 cm (A) and 100 µm (D).

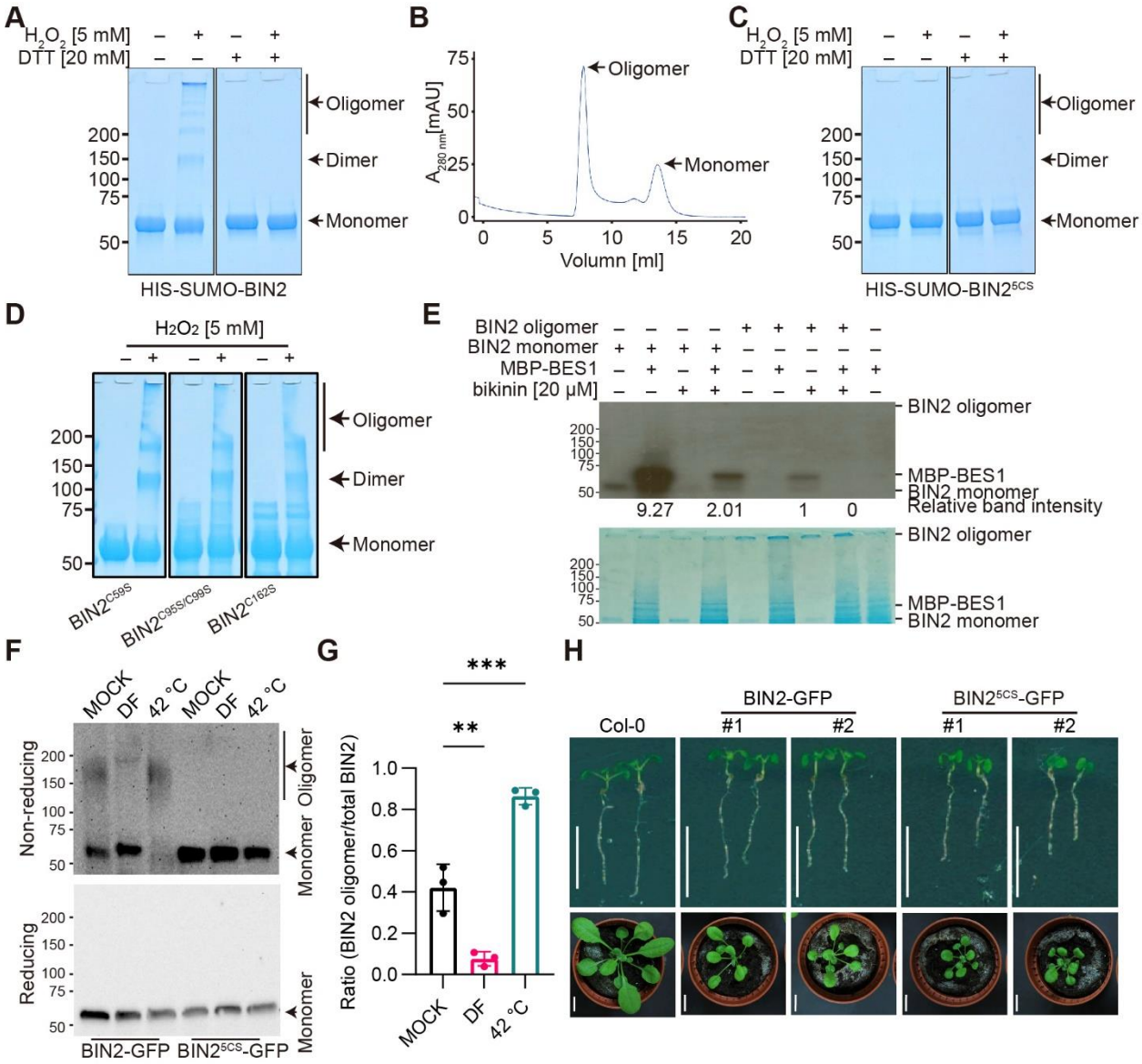

Figure 4 H_2O_2-induced BIN2 oligomerization. A, Coomassie Brilliant Blue (CBB)-stained non-reducing SDS-PAGE gel analysis of the oligomeric state of HIS-SUMO-BIN2 protein (20 μM) in the absence or presence of 20 mM dithiothreitol (DTT) and after treatment with 5 mM H_2O_2 for 30 min. B, Size-exclusion chromatography analysis of the oligomeric state of the HIS-SUMO-BIN2 protein (20 μM) after treatment with 5 mM H2O2 for 30 min. C, CBB stained SDS-PAGE gel analysis of the oligomeric state of the mutated BIN2 protein HIS-SUMO-BIN2^{5CS} (20 μM) in the absence or presence of 20 mM DTT and after treatment with 5 mM H_2O_2 for 30 min. D, CBB-stained non reducing SDS-PAGE gel analysis of the oligomeric state of HIS-SUMO-BIN2^{C59S}, HIS-SUMO-BIN2$^{C95S/C99S}$, and HIS-SUMOBIN2^{C162S} after treatment with 5 mM H_2O_2 for 30 min. E, *In vitro* kinase assay with the HIS-SUMO-BIN2 monomer and oligomer and MBP-BES1 as a substrate in the absence or presence of 10 mM bikinin (BIK). The normalized band intensities are showed. Autoradiography (top) and CBB staining (bottom). Similar results were obtained in two independent experiments. F, Immunoblot analysis of BIN2-GFP, BIN2^{5CS}-GFP. Five-day-old seedlings of *BIN2p:BIN2-GFP/bin2-3* and *BIN2p:BIN2^{C5S}-GFP/bin2-3* were treated with 100 nM deaminoformycin (DF) or H_2O (MOCK) for 24 h at 21 ℃ or heated at 42 ℃ for 1 h in liquid medium with 24 h MG132 co-treatment or pre-treatment. G, Quantification of the ratio between BIN2 oligomer and total BIN2. Bar chart shows the means, standard errors and all individual points. *P* values were compared to MOCK with one-way ANOVA with Dunnett's post hoc test, $^{**}P < 0.01$, $^{***}P < 0.001$. *n*， three independent experiments. H, Representative images of two independent *Arabidopsis* transgenic seedlings, each expressing either *BIN2p:BIN2-GFP/bin2-3* or *BIN2p:BIN2^{C5S}-GFP/bin2-3* and Col-0 grown for 12 days on agar medium (upper panel) or 25 days in soil (bottom panel). Scale bars, 1 cm.

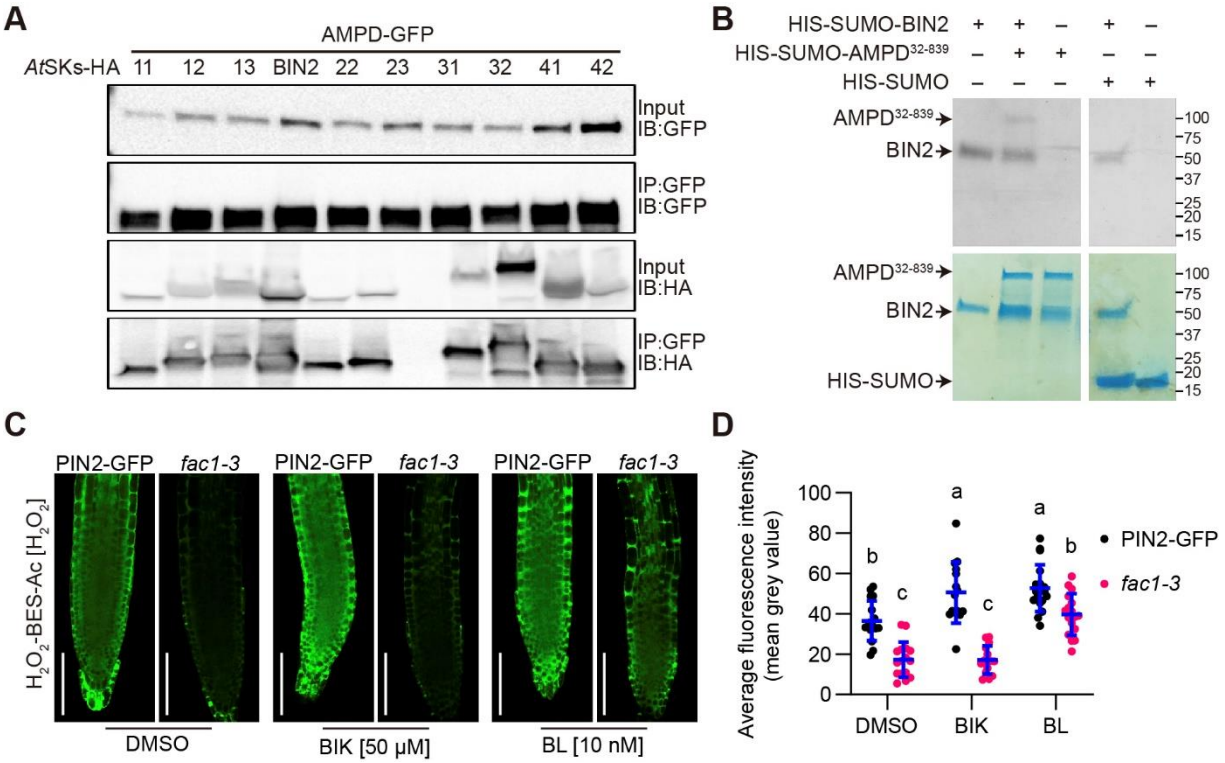

Figure 5 BIN2 regulates H_2O_2 homeostasis most likely through AMPD. A, AMPD-GFP coimmunoprecipitated with HA-tagged *At*SKs in *N. benthamiana*. AMPD-GFP was immunoprecipitated with anti-GFP Trap beads. AMPD-GFP and *At*SKs-HA were detected with an anti-GFP and anti-HA antibody, respectively. IP, immunoprecipitation; IB, immunoblot. B, *In vitro* kinase assay for HIS-SUMO-BIN2 with HIS-SUMO-AMPD$^{32-839}$ and with HIS-SUMO as negative control. Autoradiography (top) and Coomassie Brilliant Blue (CBB) staining (bottom). C, Confocal images of root tips of 5-day-old *PIN2p:PIN2-GFP*/Col-0 and *fac1-3* plants stained with H_2O_2-BES-Ac (30 min) after 24 h of treatment with 50 μM bikinin (BIK), 10 nM brassinolide (BL) and DMSO (mock). D, Quantification of fluorescent intensities in the root tips of the seedlings in (C). Scatter dot plots show all the individual points with the means and standard errors. Significant differences were determined using two-way ANOVA with Tukey's multiple comparisons test and labeled with different letters ($P < 0.05$). *n*, at least 15 seedlings from three independent experiment. *At*SK, *Arabidopsis thaliana* Shaggy/GSK3-like kinase. Scale bar, 50 μm (C).

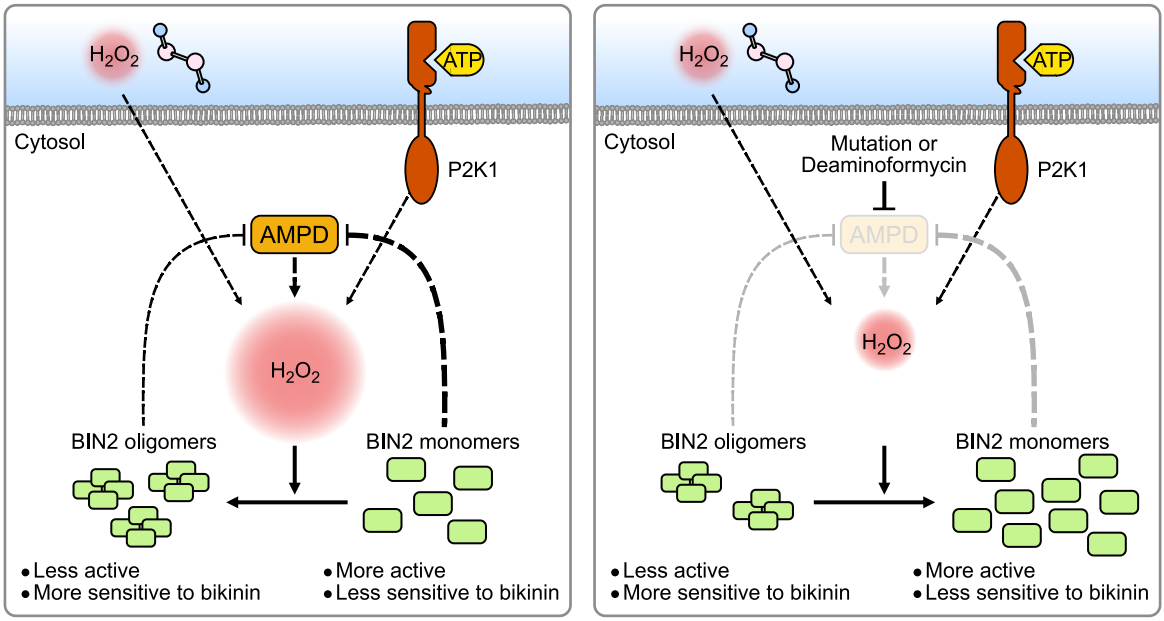

Figure 6 Model for AMPD-dependent BIN2 regulation. A, AMPD facilitates the production of reactive oxygen species (ROS) and hydrogen peroxide (H_2O_2), which induces the oligomerization of BIN2. Compared to BIN2 monomer, the oligomer is less active but more sensitive to bikinin. Moreover, BIN2 phosphorylates AMPD and probably regulates its function. The exogenous H2O2 and ATP could increase the endogenous H_2O_2 levels. B, When the AMPD function is impaired by mutation or by its chemical inhibitor deaminoformycin (DF), the amount of H2O2 is reduced, leading to the monomerization of BIN2 possible by the unknown thioredoxin. Compared to the oligomeric protein, BIN2 monomer is more active but less sensitive to bikinin, probably causing bikinin and partially BRs insensitivity in the *ampd* mutant or DF-treated wild type plants. The size of the circles for H_2O_2 indicates their levels and the size of the arrows indicates the strength of promotion or inhibition. P2K1, PURINOCEPTOR P2K1.